Meas. Sci. Technol. **20** (2009) 075105 (7pp) doi:10.1088/0957-0233/20/7/075105

Determination of global positioning system (GPS) receiver clock errors: impact on positioning accuracy

Ta-Kang Yeh[1,6], Cheinway Hwang[2], Guochang Xu[3], Chuan-Sheng Wang[4] and Chien-Chih Lee[5]

[1] Institute of Geomatics and Disaster Prevention Technology, Ching Yun University, No 229, Jiansing Rd, Jhongli 320, Taiwan
[2] Department of Civil Engineering, National Chiao Tung University, No 1001, Ta Hsueh Rd, Hsinchu 300, Taiwan
[3] GeoForschungsZentrum Potsdam, Telegrafenberg A17, 14473 Potsdam, Germany
[4] School of Mathematical and GeoSpatial Sciences, RMIT University, RMIT City Campus, GPO Box 2476 V, Melbourne, Victoria 3001, Australia
[5] General Education Center, Ching Yun University, No 229, Jiansing Rd, Jhongli 320, Taiwan

E-mail: bigsteel@cyu.edu.tw

Received 14 May 2008, in final form 14 May 2009
Published 10 June 2009
Online at stacks.iop.org/MST/20/075105

Abstract
Enhancing the positioning precision is the primary pursuit of global positioning system (GPS) users. To achieve this goal, most studies have focused on the relationship between GPS receiver clock errors and GPS positioning precision. This study utilizes undifferentiated phase data to calculate GPS clock errors and to compare with the frequency of cesium clock directly, to verify estimated clock errors by the method used in this paper. The frequency stability calculated from this paper (the indirect method) and measured from the National Standard Time and Frequency Laboratory (NSTFL) of Taiwan (the direct method) match to 1.5×10^{-12} (the value from this study was smaller than that from NSTFL), suggesting that the proposed technique has reached a certain level of quality. The built-in quartz clocks in the GPS receivers yield relative frequency offsets that are 3–4 orders higher than those of rubidium clocks. The frequency stability of the quartz clocks is on average two orders worse than that of the rubidium clock. Using the rubidium clock instead of the quartz clock, the horizontal and vertical positioning accuracies were improved by 26–78% (0.6–3.6 mm) and 20–34% (1.3–3.0 mm), respectively, for a short baseline. These improvements are 7–25% (0.3–1.7 mm) and 11% (1.7 mm) for a long baseline. Our experiments show that the frequency stability of the clock, rather than relative frequency offset, is the governing factor of positioning accuracy.

Keywords: geodetic GPS receiver, clock errors, positioning precision, allan deviation, frequency stability, relative frequency offset

(Some figures in this article are in colour only in the electronic version)

1. Introduction

The development of high-accuracy geodetic methods using dual-frequency global positioning system (GPS) carrier-phase observables has demonstrated positioning repeatability at the cm level for 1 day integrations (Zumberge *et al* 1997). However, the vertical precision of GPS is two to three times less accurate than its horizontal counterpart, mainly due to difficulties in correcting tropospheric delay, clock errors, multipath and antenna phase center variations (Rothacher

[6] Author to whom any correspondence should be addressed.

and Beutler 1998, Leick 2004). The International GNSS Service (IGS) has provided users with receiver clock errors and GPS satellite clock errors via internet to improve positioning accuracy (Ray and Senior 2005). Timing of a GPS receiver is an important factor affecting positioning accuracy. In a study by Yeh *et al* (2007), a 1–2 cm positioning error was found due to improperly modeled receiver clock errors. In GPS positioning, receiver clock errors are considered systematic errors that can be reduced by differencing the GPS code and phase observables. However, for researchers interested in time and frequency standards, GPS observables can also be used to determine relative frequency offset and frequency stability. Time transfer by GPS is popular in many laboratories in the world, e.g., Bureau International des Poids et Mesures (BIPM). Using rapid orbits and final orbits of GPS, the Astronomical Institute of the University of Berne (AIUB) has cooperated with the Swiss Federal Office of Metrology and Accreditation (METAS) to provide time transfer service with a ns level accuracy (Dach *et al* 2003). Ray and Senior (2003) show that GPS time transfer can reach a precision of about 100 ps at each epoch in favorable cases. However, on average the absolute time transfer capability is limited to >1 ns, due to uncertainties in instrumental calibrations (Petit *et al* 2001).

The performance of a GPS receiver can be assessed by comparing the coordinates obtained with the receiver with given, sufficiently accurate coordinates at a calibration site. In Taiwan, the Taiwan National Measurement Laboratory (TNML) of the Industrial Technology Research Institute (ITRI) has established a GPS calibration network, which is tied to the International Terrestrial Reference Frame 2000 (ITRF 2000, Altamimi *et al* 2002). In addition to coordinate comparison, the method of frequency calibration is also a feasible method for assessing the quality of a GPS receiver (Yeh *et al* 2006). Moreover, the GPS time in some of the receivers has been found to have some bias error. This requires a calibration of the GPS receiver prior to its precise application (Banerjee *et al* 2007). Aiming at improving the precision and reliability of GPS relative positioning, this study utilizes undifferentiated phases collected mainly at TNML to determine receiver clock errors and to compare the performances of a quartz clock and a rubidium clock ready at TNML. The relationship between receiver clock error and GPS positioning accuracy is also investigated.

2. Collection of GPS data

The main GPS data used in this paper were collected at the TNML tracking station, which is also a station in the IGS network and receives continuous GPS data. This GPS station is located on the top floor of a building that houses the Center for Measurement Standards (CMS) of ITRI. The GPS receiver is an Allen Osborne Associates (AOA) BenchMark with an AOAD/M choke ring antenna. In a regular mode, the quartz clock and the clock steering function of this receiver are turned off, and the frequency source is based on a Datum 8040A rubidium clock. The frequency of this rubidium clock may change over time, so a regular frequency calibration is made. For the experiments in this paper, this rubidium clock was sent to the National Standard Time and Frequency Laboratory (NSTFL) of Taiwan on 5 May (DOY 125) 2005 for calibration. The built-in quartz clock and its clock steering function were turned on again. The clock steering uses GPS observations to synchronize the time of the quartz clock with the times from the cesium and rubidium clocks of GPS satellites (Allen Osborne Associates 1997). On 13 May 2005, the calibration of the rubidium clock was completed, and it replaced the quartz clock again at TNML. Table 1 summarizes the GPS data collected at TNML with respect to the quartz and rubidium clocks. Hereafter the three GPS observation periods (before, during and after the calibration) are named sessions 1, 2 and 3.

Table 1. GPS observations obtained at the TNML tracking station.

Session	DOY in 2005	Frequency source
1	118–124	Rubidium clock
2	126–132	Quartz clock
3	134–140	Rubidium clock

To determine the frequency offset and frequency stability of a receiver clock, a reference (standard) clock is needed. This reference clock is assumed to be free from offset. In this study, the frequency of a HP 5071A cesium clock at the TWTF GPS station is adopted as the reference clock. TWTF is located 25 km from TNML and is operated by the NSTFL in Yangmei, Taiwan. TWTF is a continuous GPS station with an Ashtech Z-XII3T receiver and an ASH701945 C_M choke ring antenna. This HP 5071A cesium clock serves as an external clock for the GPS receiver at TWTF. The coordinates of TWTF were held fixed when computing the coordinates of TNML by GPS relative positioning. The repeatabilities of the TNML coordinates based on 7 days of GPS data were determined for the three sessions listed in table 1.

During the 21 days in table 1, the temperature, humidity and pressure were recorded and the qualities of GPS observations were analyzed using the TEQC software. TEQC is developed by the University Navstar Consortium and can be used to convert the binary receiver format to the standard Receiver Independent Exchange (RINEX) format, edit existing RINEX files, and check the data quality (Estey and Meertens 1999). Since there are no major changes in the environmental records and the quality indices of the observations, the positioning accuracies at TNML are governed by the receiver clocks used. That is, the relative frequency offset and frequency stability of clock will be the dominating factors for the coordinate variation.

3. Assessment of relative frequency offset and frequency stability

In this paper, undifferentiated GPS phase observables (no time differences, satellite differences and receiver differences) are used to calculate relative frequency offsets and frequency stabilities of the GPS receivers, based on the method of Dach *et al* (2003). This is called the indirect method of frequency calibration, in comparison to the direct method of frequency calibration using a HP 5071A cesium clock (see below). Figure 1 shows the geometry and principle for determining

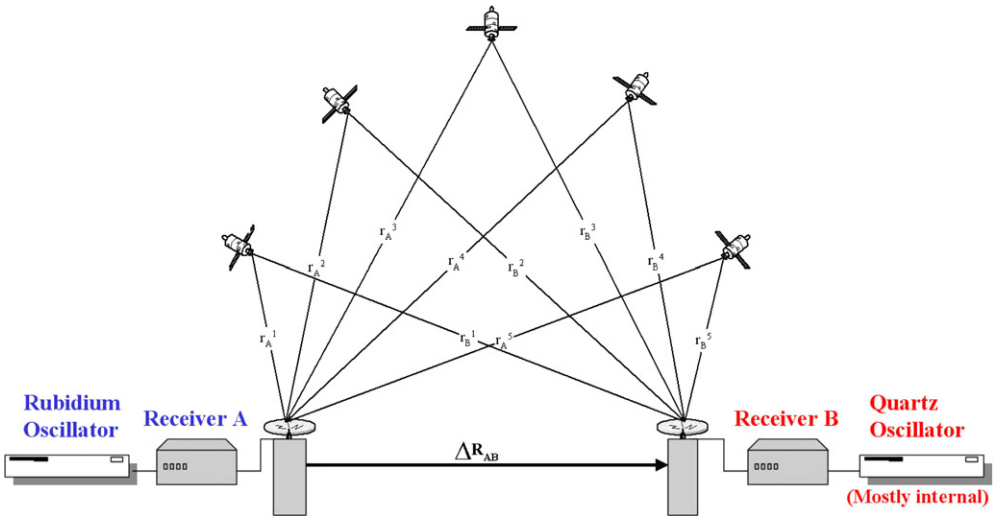

Figure 1. The geometry and principle of the determination of the receiver clock errors.

relative frequency offset and frequency stability in a baseline involving two receivers (A and B). The difference between the clock error of a receiver and that of a GPS satellite is to be determined. The clock of receiver A (a rubidium clock) is regarded as a reference clock. The observation equation of a GPS pseudorange from station i to satellite k can be expressed as (Dach *et al* 2003, Leick 2004)

$$P_i^k = \left|\vec{\rho}^k\left(t-\omega_i^k\right)-\vec{\rho}_i\left(t\right)\right| - c\cdot\left(\delta_0^k+\delta^k\left(t\right)\right) + I_i^k + T_i^k + c\cdot\left(\delta_{i0}+\delta_i\left(t\right)\right) + e_i^k, \quad (1)$$

where P_i^k is the pseudorange observation, $\vec{\rho}^k(t-\omega_i^k)$ is the position vector of satellite k at transmission time $(t-\omega_i^k)$, ω_i^k is the signal travel time, $\vec{\rho}_i\,(t)$ is the position vector of station i at receiving time t, c is the speed of light, δ_0^k is the hardware delay of satellite k (constant), $\delta^k\,(t)$ is the satellite clock error at t, I_i^k is the signal delay due to ionosphere, T_i^k is the signal delay due to troposphere, δ_{i0} is the hardware delay in the receiver i (constant), $\delta_i(t)$ is the receiver clock error at t and e_i^k is the random error of pseudorange.

The observation equation of a GPS carrier phase is

$$\Phi_i^k = \left|\vec{\rho}^k\left(t-\omega_i^k\right)-\vec{\rho}_i\left(t\right)\right| - c\cdot\left(\delta_0^k+\delta^k\left(t\right)\right) - I_i^k + T_i^k + c\cdot\left(\delta_{i0}+\delta_i\left(t\right)\right) + \lambda N_i^k + \varepsilon_i^k, \quad (2)$$

where Φ_i^k is the phase observation, λ is the wave length, N_i^k is the initial phase ambiguity and ε_i^k is the random noise of phase. When using phase observations, the estimated ambiguity N_i^k will absorb hardware delays (δ_0^k and δ_{i0}). According to Dach *et al* (2003), it is not likely to separate the initial phase ambiguity from the receiver and satellite hardware delays using phase observations alone, and pseudorange observations must be used to de-correlate them.

We used the Bernese version 4.2 software (Beutler *et al* 2001) to process GPS data and estimate the receiver clock errors. Since the use of differenced observables may eliminate systematic errors and signals of interest, we decide to use undifferentiated observables to estimate clock errors. To use undifferentiated observables, data cleaning is necessary and was carried out before parameter estimations. The input to the program for data cleaning, which stands for RINEX smoothing, is a single RINEX file. The output is a RINEX file again, hopefully free from outliers and cycle slips. A summary of the actions taken by the program is contained in the output of Bernese 4.2. Each RINEX file is processed satellite by satellite. The observations of each satellite are pre-processed in the following steps:

(1) Screening of the Melbourne–Wübbena linear combination of phase for outliers and cycle slips.
(2) The geometry-free linear combination of phase is examined to determine the size of cycle slips in L1 and L2. This information is used to repair the observations for cycle slips.
(3) Screening of the difference between the ionosphere-free linear combinations of phase and code observations, to remove bad observations which were not detected in step 1.
(4) Smoothing codes using the screened observations.

For code smoothing, we have to account for the opposite sign of the ionospheric effect for the code and phase observations. The smoothed code at epoch t may then be written as (Beutler *et al* 2001)

$$\tilde{P}_1(t) = \Phi_1(t) + \bar{P}_1 - \bar{\Phi}_1 + 2\frac{f_2^2}{f_1^2-f_2^2} \times\left[\left(\Phi_1(t)-\Phi_2(t)\right)-\left(\bar{\Phi}_1-\bar{\Phi}_2\right)\right] \quad (3)$$

$$\tilde{P}_2(t) = \Phi_2(t) + \bar{P}_2 - \bar{\Phi}_2 + 2\frac{f_1^2}{f_1^2-f_2^2} \times\left[\left(\Phi_1(t)-\Phi_2(t)\right)-\left(\bar{\Phi}_1-\bar{\Phi}_2\right)\right], \quad (4)$$

where $\tilde{P}_F(t)$ is the smoothed code measurement at epoch t and frequency F, $\Phi_F(t)$ is the carrier-phase measurement at epoch t and frequency F, $\bar{P}_F-\bar{\Phi}_F$ is the mean difference between all the accepted code and phase measurements in the current observation arc on frequency F, $\Phi_1(t)-\Phi_2(t)$ is ionospheric delay at the current epoch and $\bar{\Phi}_1-\bar{\Phi}_2$ is mean ionospheric delay over all the accepted phase measurements in the current observation arc.

Table 2. Relative frequency offset and frequency stability of the rubidium clock at TNML.

Session 1 (rubidium clock)			Session 3 (rubidium clock)		
DOY	Relative frequency offset	30 s frequency stability	DOY	Relative frequency offset	30 s frequency stability
118	6.57×10^{-10}	3.98×10^{-12}	134	6.54×10^{-10}	3.01×10^{-11}
119	6.57×10^{-10}	3.75×10^{-12}	135	6.55×10^{-10}	4.56×10^{-12}
120	6.58×10^{-10}	3.54×10^{-12}	136	6.56×10^{-10}	2.94×10^{-12}
121	6.58×10^{-10}	3.27×10^{-12}	137	6.57×10^{-10}	3.14×10^{-12}
122	6.59×10^{-10}	3.08×10^{-12}	138	6.57×10^{-10}	3.75×10^{-12}
123	6.59×10^{-10}	4.11×10^{-12}	139	6.57×10^{-10}	3.53×10^{-12}
124	6.59×10^{-10}	3.47×10^{-12}	140	6.59×10^{-10}	3.25×10^{-12}
Average	6.58×10^{-10}	3.60×10^{-12}	Average	6.57×10^{-10}	3.53×10^{-12}

After obtaining the clock errors of the GPS receiver from the undifferentiated phases, the clock errors of each epoch were used to compute the relative frequency offset and frequency stability. However, an atomic clock frequency may drift; we choose to compute the modified Allan deviation (Allan and Weiss 1980, Lesage and Ayi 1984) to determine the frequency stability $\bar{\sigma}_y$ as follows:

$$\bar{\delta}_i(t) = [\delta_i(t+1) + \delta_i(t)]/2 \tag{5}$$

$$\bar{y}'_t = [\bar{\delta}_i(t+2) - \bar{\delta}_i(t)]/\tau \tag{6}$$

$$\bar{\sigma}_y(\tau) = \left[\frac{1}{2(N-3m+1)} \sum_{t=1}^{N-3m+1} \left(\bar{y}'_{t+m} - \bar{y}'_t\right)^2\right]^{1/2}, \tag{7}$$

where $\delta_i(t)$ is the time residual measurement (receiver clock error, see equations (1) and (2)), $\bar{\delta}_i(t)$ is the average value of every two neighboring measurements, τ is the sampling interval, N is the number of time samples and m is the step size corresponding to the sampling interval (τ).

The frequency stabilities were determined in the three sessions. Table 2 shows daily relative frequency offsets and frequency stabilities. Note that a small fluctuation of temperature occurred on DOY 134 when the rubidium clock was just re-installed, but this fluctuation did not affect the overall result in table 2.

Next we use the HP 5071A cesium clock of the NSTFL to evaluate the rubidium clock. This is the direct method of frequency calibration. A counter was used to record the frequency offsets between the rubidium clock and the HP 5071A cesium clock. We compared these measurements and concluded the rubidium clock has a relative frequency offset of 6.6×10^{-10} and frequency stability of 5.0×10^{-12}. The relative frequency offset and frequency stability from this comparison agree very well with those given in table 2, suggesting that our data processing method is effective and the method of modified Allan deviation for the determination of frequency stability (equation (7)) is adequate. Table 3 shows the relative frequency offset and frequency stability of the quartz clock obtained during the calibration period. The relative frequency offset of the quartz clock is four orders of magnitude better than that of the rubidium clock. However, the frequency stability of the rubidium clock is two orders of magnitude better than the quartz clock.

We also analyzed the daily frequency changes of the quartz clock and the rubidium clock. Figure 2 shows the relative frequency offsets of the quartz clock relative to the rubidium clock on DOY 126. Since the AOA BenchMark GPS receiver has synchronized its time with the GPS time (clock steering), the relative frequency offsets oscillate around zero with a mean value of about 7.75×10^{-14}. Figure 3 shows the frequency stabilities of the quartz clock on DOY 126. The stability improves with time. Since clock steering was activated, the frequency stabilities of the quartz clock are mainly due to external noises. Figure 4 shows the relative frequency offsets of the rubidium clock on DOY 118. The offsets vary linearly with time, and this is typical of a rubidium clock. The mean offset is 6.57×10^{-10} and the rate is less than 1×10^{-10}/year. Because the offset of the quartz clock is compensated by clock steering, it is better than that of the rubidium clock. Figure 5 shows the frequency stabilities of the rubidium clock on DOY 118, which are on average about 100 times better than those of the quartz clock (figure 3). For example, at the 30th second, the frequency stabilities of the rubidium and quartz clocks are 3.98×10^{-12} and 1.02×10^{-10}, respectively.

Table 3. The relative frequency offset and frequency stability of the quartz clock at TNML.

Session 2 (quartz clock)		
DOY	Relative frequency offset	30 s frequency stability
126	7.75×10^{-14}	1.02×10^{-10}
127	3.90×10^{-14}	9.93×10^{-11}
128	6.05×10^{-14}	1.03×10^{-10}
129	5.69×10^{-14}	1.06×10^{-10}
130	6.51×10^{-14}	1.06×10^{-10}
131	9.93×10^{-15}	1.04×10^{-10}
132	5.71×10^{-14}	1.04×10^{-10}
Average	5.23×10^{-14}	1.03×10^{-10}

4. Accuracy assessment of static relative positioning using a short baseline

To better understand the error characteristics of the quartz and rubidium clocks, we also assess the accuracies of GPS static relative positioning based on the two clocks. Again, we used the observations collected in three sessions of table 1 to carry out static relative positioning between TNML and TWTF, which is considered a short baseline. We used Bernese 4.2 software to process the double-differenced phases for

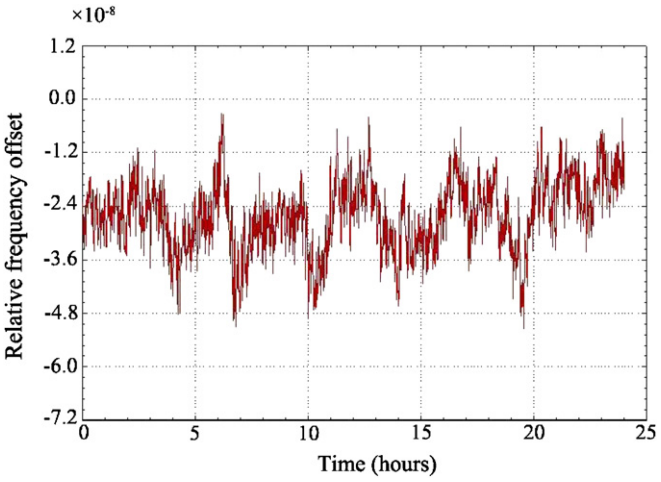

Figure 2. Relative frequency offsets of the quartz clock on DOY 126.

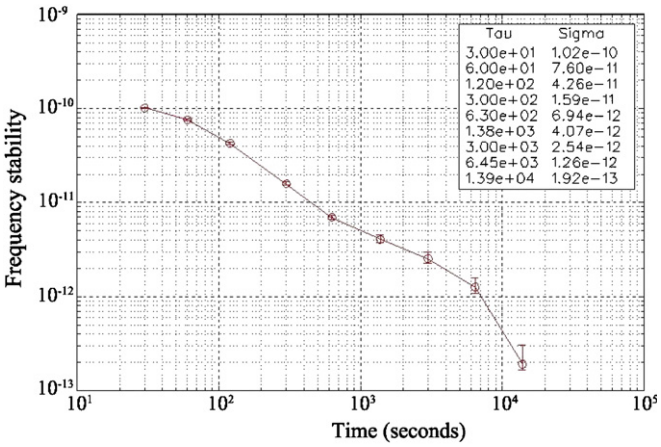

Figure 3. Frequency stabilities of the quartz clock on DOY 126.

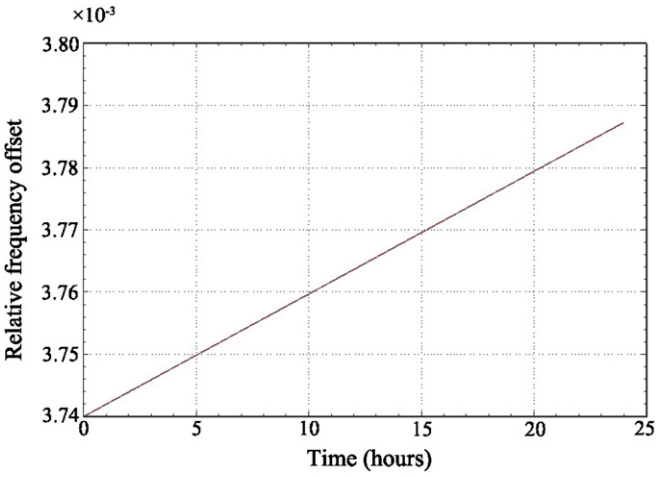

Figure 4. Relative frequency offsets of the rubidium clock on DOY118.

the relative positioning. Phase ambiguities were solved and kept fixed to integer values. Precise IGS satellite orbits were used and a cut-off angle of 15° was adopted. Pole tide, solid earth tide and ocean tide loading corrections were

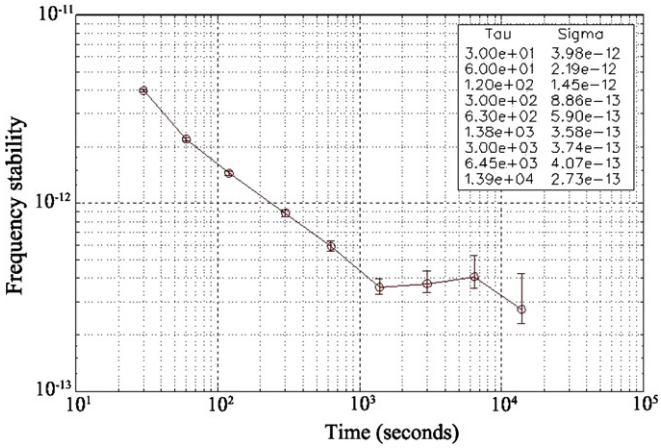

Figure 5. Frequency stabilities of the rubidium clock on DOY 118.

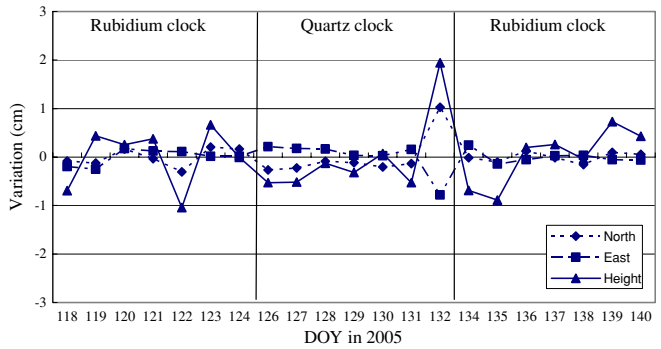

Figure 6. Position errors of three-dimensional coordinates at TNML obtained from the static relative positioning before, during and after the calibration.

applied to the GPS data. Different strategies for reducing tropospheric delays have been tested, and an optimal strategy is adopted as follows. With the ionosphere-free combination of phase, we first estimated zenith delay parameters for each day using the Saastamoinen *a priori* delay and the $1/\cos(Z)$ mapping function, where Z is the zenith angle. Then, the site coordinates were corrected for the effect of tropospheric delay by applying the estimated zenith delay parameters (Yeh *et al* 2008). When calculating the coordinates of TNML, the coordinates of TWTF were held fixed. The averages of all coordinate components were determined and removed from the original coordinates to compute the coordinate variations in the three sessions. Figure 6 shows the variations of the three coordinate components.

The standard deviation of coordinate variations is now considered a descriptor of positioning accuracy. The standard deviations corresponding to the three sessions are given in table 4. The performance of the rubidium clock remains the same when re-installing it to the GPS receiver, as suggested by the consistency between the standard deviations from sessions 1 and 3 in table 4. Use of the rubidium clock (both before and after the calibration) has led to a better coordinate repeatability (i.e., small standard deviation) than the quartz clock in the relative static positioning. The result of this experiment suggests that the frequency stability governs the accuracy of GPS relative positioning. Specifically, compared

Table 4. Standard deviations of coordinate variation (in mm) at three sessions.

	Session 1 (rubidium clock)	Session 2 (quartz clock)	Session 3 (rubidium clock)
North	1.9	4.6	1.0
East	1.6	3.5	1.2
Height	6.3	8.9	5.9

to the quartz clock, the rubidium clock has a better frequency stability, which yields smaller coordinate variations. This can be explained as follows. A clock error, δ, can be expressed as a function of time, t, as

$$\delta = a_0 + a_1(t - t_{oe}) + a_2(t - t_{oe})^2, \quad (8)$$

where t_{oe} is a reference epoch, and a_0, a_1 and a_2 represent bias, drift and drift rate, respectively. The frequency offset may be responsible for the clock bias (a_0), but other kinds of error sources may contribute as well, e.g., signal delay due to atmosphere, hardware delay in the receiver and random noise. Despite this, this kind of error can be reduced or removed using GPS data processing, e.g., single differencing and double differencing. Therefore, the frequency offset has little impact on positioning accuracy. On the other hand, the drift (a_1) and the drift rate (a_2) terms associated with the frequency stability cannot be reduced by differencing GPS phases. Therefore, the frequency stability is a key factor for positioning accuracy.

5. Analyses using long data records and long baselines

To confirm the results given in sections 3 and 4, we collected GPS data from DOY 141–170, 2002, using the quartz clock as the frequency source, and then collected GPS data from DOY 172–205, 2002, using the rubidium clock as the frequency source, both at the TNML station of ITRI. We repeat the same analyses as those given in sections 3 and 4. During these two periods, we also obtained GPS data at TWTF and WUHN (Wuhan, China). WUHN is a station in the IGS network. The lengths of the TNML–TWTF baseline and the TNML–WUHN baseline are 25 and 920 km, respectively. Again, we used undifferentiated GPS phases to calculate receiver clock errors, which were then used to determine the relative frequency offsets and frequency stabilities of the quartz and rubidium clocks (figure 7). The results in figure 7 are consistent with those given in tables 2 and 3, which are based on 1 week of GPS data. Figure 7 shows that the relative frequency offset of the quartz clock is three orders of magnitude better than that of the rubidium clock because of the clock steering, and the frequency stability of the quartz clock is two orders of magnitude worse than the rubidium clock.

These 2 months of GPS data were also used to assess the accuracy of static relative positioning. Again, temperature, humidity and pressure data near TNML were collected. The quality of GPS data was examined by the TEQC software to remove outliers. There were no major changes of temperature, humidity and pressure during the two sessions of GPS data collection. Therefore, the differences in the

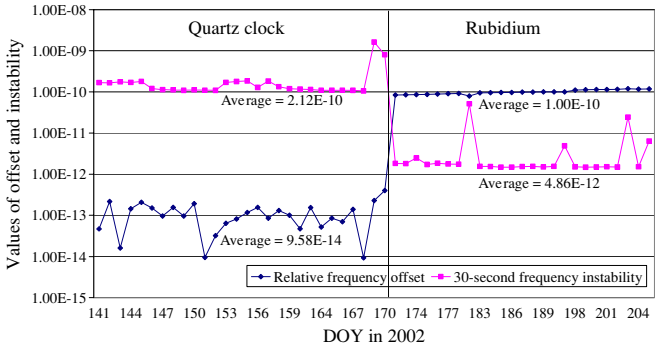

Figure 7. The relative frequency offset and frequency stability at TNML in year 2002.

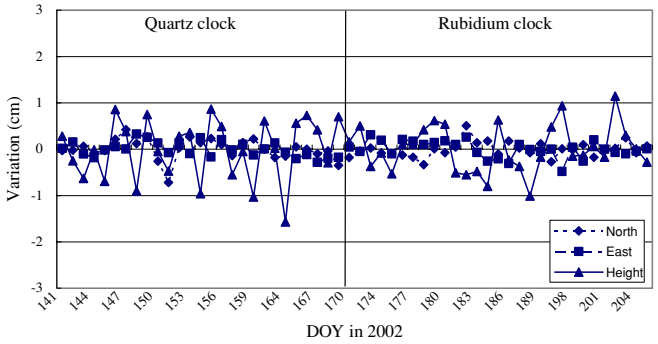

Figure 8. Position errors of three-dimensional coordinates of the short-distance static relative positioning in year 2002.

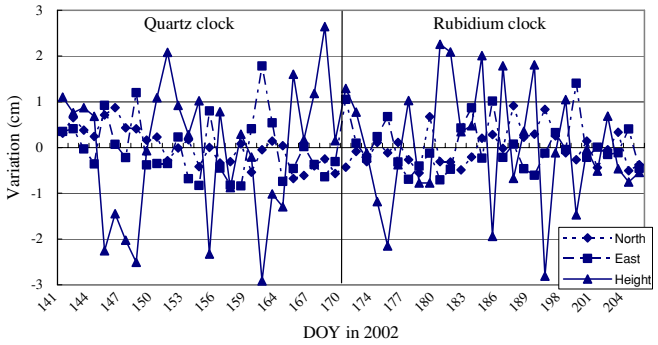

Figure 9. Position errors of three-dimensional coordinates of long-distance static relative positioning in year 2002.

results of static relative positioning are mainly due to different frequency sources (quartz and rubidium clocks), rather than environmental changes. Daily solutions of the short TNML–TWTF baseline and the long TNML–WUHN baseline were obtained using Bernese 4.2 and the same procedures as those given in section 4. Figures 8 and 9 show the coordinate variations and the standard deviations of the variations from the TNML–TWTF and TNML–WUHN baseline solutions, respectively. Table 5 lists the standard deviations of the coordinate variations. Again, the rubidium clock leads to smaller coordinate variations than the quartz clock, which is consistent with the result given in section 4. From table 5, use of the rubidium clock results in more reduction

Table 5. Standard deviations of coordinate variation (in mm) for short and long baselines using the quartz and rubidium clocks.

	Short baseline (TNML–TWTF)		Long baseline (TNML–WUHN)	
	Quartz clock	Rubidium clock	Quartz clock	Rubidium clock
North	2.3	1.7	4.2	3.9
East	1.6	1.9	6.9	5.2
Height	6.5	5.2	14.8	13.1

of coordinate variation for the short baseline than for the long baseline.

6. Conclusions

The frequency offset of the rubidium clock as computed by the method in this paper (the indirect method, see section 3) is consistent with that from a direct comparison of the rubidium clock with the HP 5071A cesium clock (the direct method), despite a mean difference of 1.5×10^{-12} in the frequency stability between the two methods. The quartz clock's relative frequency offset is small due to clock steering that synchronizes the receiver clock time and GPS time. However, the frequency stability of the quartz clock is degraded progressively due to time resetting. In one experiment, we turned off clock steering of the rubidium clock, and the result is that the rubidium clock's relative frequency offset became increasingly large but its frequency stability remained small. When changing the frequency source from the quartz clock to the rubidium clock in the GPS baseline solutions between TNML and TWTF (25 km), the positioning accuracy is improved by 26–78% (0.6–3.6 mm) in the horizontal coordinate components, and 20–34% (1.3–3.0 mm) in the vertical component. For the long baseline (YNML–WUHN, 920 km), the maximum improvements in the horizontal and vertical components are 7–25% (0.3–1.7 mm) and 11% (1.7 mm), respectively.

The quality of the frequency source (in terms of frequency stability) has a greater impact on GPS positioning accuracy for a short baseline than for a long baseline. The likely reason is that the error sources in the short baseline positioning are mostly reduced or removed due to differencing of GPS observables, so that the frequency source becomes the dominant factor on positioning accuracy. In the case of long baseline, differencing of GPS observables cannot remove systematic errors such as tropospheric and ionospheric delays and these remaining errors still dominate positioning accuracy, leaving the impact of changing frequency source less dominant but still influential. In summary, a better receiver clock (in terms of frequency stability) leads to a better GPS positioning accuracy. As future work, we recommend a scenario where two receivers of the same type share the same antenna but use two different clocks (e.g., a quartz clock and a rubidium clock). This would make the result insensitive to GPS satellite constellations and environmental factors such as temperature and pressure.

Acknowledgments

The authors would like to thank the National Science Council of the Republic of China, Taiwan, for financially supporting this research, under contract no NSC94–2218-E-231–001.

References

Allan D and Weiss M 1980 Accurate time and frequency transfer during common-view of a GPS satellite *Proc. 1980 IEEE Frequency Control Symp. (Philadelphia)* pp 334–56

Allen Osborne Associates 1997 *User Manual—The TurboRogue Family of GPS Receivers* ITT Aerospace/Communications Division, Westlake Village, CA

Altamimi Z, Sillard P and Boucher C 2002 ITRF2000: a new release of the International Terrestrial Reference Frame for earth science applications *J. Geophys. Res.* **107** 2214

Banerjee P, Suman, Suri A K, Chatterjee A and Bose A 2007 A study on the potentiality of the GPS timing receiver for real time applications *Meas. Sci. Technol.* **18** 3811–5

Beutler G *et al* 2001 *Bernese GPS Software Version 4.2.* Astronomical Institute, University of Bern

Dach R, Beutler G, Hugentobler U, Schaer S, Schildknecht T, Springer T, Dudle G and Prost L 2003 Time transfer using GPS carrier phase: error propagation and results *J. Geodesy* **77** 1–14

Estey L H and Meertens C M 1999 The multi-purpose toolkit for GPS/GLONASS data *GPS Solutions* **3** 42–9

Leick A 2004 *GPS Satellite Surveying* (Hoboken, NJ: Wiley)

Lesage P and Ayi T 1984 Characterization of frequency stability: analysis of the modified Allan variance and properties of its estimate *IEEE Trans. Instrum. Meas.* **IM-33** 332–6

Petit G, Jiang Z, White J, Beard R and Powers E 2001 Absolute calibration of an Ashtech Z12-T GPS receiver *GPS Solutions* **4** 41–6

Ray J and Senior K 2003 IGS/BIPM pilot project: GPS carrier phase for time/frequency transfer and time scale formation *Metrologia* **40** 270–88

Ray J and Senior K 2005 Geodetic techniques for time and frequency comparisons using GPS phase and code measurements *Metrologia* **42** 215–32

Rothacher M and Beutler G 1998 The role of GPS in the study of global change *Phys. Chem. Earth* **23** 1029–40

Yeh T K, Liou Y A, Wang C S and Chen C S 2008 Identifying the degraded environment and bad receivers setting by using the GPS data quality indices *Metrologia* **45** 562–70

Yeh T K, Wang C S, Lee C W and Liou Y A 2006 Construction and uncertainty evaluation of a calibration system for GPS receivers *Metrologia* **43** 451–60

Yeh T K, Wang C S, Chao B F, Chen C S and Lee C W 2007 Automatic data-quality monitoring for continuous GPS tracking stations in Taiwan *Metrologia* **44** 393–401

Zumberge J F, Heflin M B, Jefferson D C, Watkins M M and Webb F H 1997 Precise point positioning for the efficient and robust analysis of GPS data from large networks *J. Geophys. Res.* **102** 5005–17